Solar Energy Materials and Solar Cells 182 (2018) 98–104

Contents lists available at ScienceDirect

Solar Energy Materials and Solar Cells

journal homepage: www.elsevier.com/locate/solmat

Light and elevated temperature induced degradation in p-type and n-type cast-grown multicrystalline and mono-like silicon

Hang Cheong Sio[a,*], Haitao Wang[b], Quanzhi Wang[b], Chang Sun[a], Wei Chen[b], Hao Jin[b], Daniel Macdonald[a]

[a] Research School of Engineering, The Australian National University, Australia
[b] Jinko Solar Co., Ltd., China

ARTICLE INFO

Keywords:
LID
LeTID
Degradation
Regeneration
Multicrystalline silicon
Mono-like silicon

ABSTRACT

We compare light induced degradation behaviours in lifetime samples and fully fabricated solar cells made from p-type boron-doped high performance multicrystalline silicon, p-type boron-doped mono-like silicon, n-type phosphorus-doped high performance multicrystalline silicon and p-type boron-doped Czochralski-grown silicon. Our results confirm that the degradation in multicrystalline silicon is triggered by the rapid cooling after the firing process. All cast-grown silicon samples subjected to fast cooling show lifetime reduction after light soaking. Interestingly, the degradation rate in n-type multicrystalline silicon is found to be orders of magnitude slower than in p-type multicrystalline silicon, suggesting that the defect formation mechanism could be affected by the positions of the quasi fermi levels.

1. Introduction

Solar cells made from multicrystalline silicon (mc-Si) suffer from an unexpectedly strong light induced degradation (LID) phenomenon that cannot be attributed to the boron-oxygen (BO) complex [1–3] commonly observed in p-type boron-doped Czochralski-grown silicon (Cz-Si). This degradation effect is commonly referred as light and elevated temperature induced degradation (LeTID), since the degradation measurements are typically performed at a higher temperature to accelerate the reaction, which otherwise occurs too slowly to be measured within a reasonable time scale at room temperature. Solar cells based on the passivated emitter and rear cell (PERC) structure are reported to be particularly affected by this degradation [4–8]. A performance loss of up to 7% at the module level is estimated within the first 3 years after installation [9].

The root cause for the degradation remains unclear to date. Studies have linked LeTID to the high temperature processing steps in solar cell fabrication [7,10–14]. Bredemeier et al. [12] compared mc-Si wafers fired at 900°C and 650°C, and only observed severe lifetime degradation in wafers fired at 900°C. Chan et al. [10] suggested that substantial LeTID can only be triggered if the peak firing temperature exceeds 700 °C, and can be largely reduced by incorporating an additional firing step at a reduced temperature afterwards. Eberle et al. [14] showed that wafers that were subjected to a fast firing process exhibit significantly stronger degradation than wafers subjected to the same peak firing temperature, but with slower heating and cooling rates. Zuschlag et al. [13] demonstrated that non-gettered wafers are more sensitive to LeTID compared to gettered samples. Moreover, it has been found that the rate and extent of the degradation depends not only on temperature [15], but also on the carrier injection level [16], which is influenced by the operating conditions [17,18] (e.g. open-circuit, short-circuit and maximum power point) and the illumination intensity [15,19]. In addition, recent works [20] have reported that the degradation can also be induced by dark annealing at elevated temperature, even without the presence of light.

Various solutions have been proposed to mitigate LeTID. One strategy is to prevent LeTID by adapting solar cell fabrication processes, such as applying a lower peak firing temperature [7,10,12], changing the firing profile [10,14], or rearranging the processing sequence [17,18]. These methods are effective in avoiding LeTID, but often require significant modifications in the processing which may not be feasible for industrial production. Another strategy is to erase the impact of LeTID by activating and accelerating the regeneration process that occurs after the degradation, through annealing the solar cells at higher temperature with stronger illumination [10,19,21,22], or under biased conditions [17,18]. These methods have proven to be effective in passivating LID caused by BO defects [23], but may not be so successfully applied on LeTID, due to its slow reaction rate and the uncertain long-term stability of the regenerated cells.

In addition to p-type mc-Si, some very recent works have observed

* Corresponding author.
E-mail address: kelvin.sio@anu.edu.au (H.C. Sio).

https://doi.org/10.1016/j.solmat.2018.03.002
Received 14 August 2017; Received in revised form 27 February 2018; Accepted 1 March 2018

similar degradation activities in p-type boron-doped Cz-Si [20,24] and float-zone Si [25–27] when illuminated at elevated temperature. In this paper, we will compare the degradation kinetics on three types of cast-grown Si materials, namely p-type boron-doped high performance (HP) mc-Si, p-type boron-doped mono-like Si and n-type phosphorus-doped HP mc-Si. Also grown by directional solidification, mono-like Si contains similar amounts of metal impurities compared to mc-Si, but features a distinct crystallographic structure [28,29], making it a suitable material for investigating the possible roles of metal impurities, grain boundaries and crystal dislocations in LeTID. On the other hand, n-type mc-Si does not contain boron, hence is not affected by BO defects and iron-boron (Fe-B) pairing reactions [30]. Furthermore, the use of n-type material may reveal any influence of the position of the quasi fermi levels on LeTID, which may in turn provide additional insights into the origins of the defects responsible for the degradation.

2. Experimental methods

Cast-grown wafers studied in this work were cut from the middle section of a central brick of a p-type boron-doped HP mc-Si ingot, an n-type phosphorus-doped HP mc-Si ingot and a p-type boron-doped mono-like Si ingot respectively. All ingots were cast in industrial G6 crucibles. The p-type and n-type HP mc-Si ingot were grown by the same manufacturer, whereas the mono-like Si ingot was produced by a second manufacturer. P-type boron-doped Cz-Si wafers were also included in the study as a reference. All wafers were around $200\mu m$ thick before processing. Table 1 summarises the resistivity and the interstitial oxygen concentration measured with Fourier Transform Infrared Spectroscopy (FTIR) for the studied wafers.

The wafers were processed into lifetime test structures, based on a PERC fabrication process without the metallisation step, in an industrial production line. The cell process involves texturing, $POCl_3$ diffusion, rear-side etch and surface passivation. The p-type samples feature plasma enhanced chemical vapour deposition (PECVD) SiN_x films on the front surfaces, and Al_2O_3/SiN_x stacks on the rear surfaces. The n-type samples feature PECVD SiN_x films on both front and rear surfaces. The samples were then divided into four groups and fired under different conditions. Wafers from group A were non-fired control samples. Wafers from group B were fired in an industrial conveyor-belt furnace in a cell production line, with a peak temperature of approximately 700°C. Wafers from group C and D were annealed in a rapid thermal processing (RTP) furnace at an actual temperature of 700°C for 5 s (as measured by a thermocouple attached to the sample), followed by different ramp-down rates ($20°C/s$ for the slow-cooled samples and $65-85°C/s$ for the fast-cooled samples). The reported cooling rate is the average cooling rate between 700°C and 400°C. An identical ramp-up rate ($20°C/s$) was applied to all RTP-processed wafers.

Additional samples were prepared to evaluate the influence of surface passivating films on the degradation properties. The samples received similar treatments as the n-type samples mentioned above. After surface passivation, all wafers were fired in an industrial conveyor-belt furnace, then had the dielectric films and the n + layers removed via HF dip. Afterwards, the wafers were chemically polished, separated into two series, and re-coated with two different dielectric films for surface passivation. Wafers from the first series were coated with SiN_x deposited using a Roth & Rau AK400 PECVD system. The wafers were heated with a ramp-up rate of around $10°C/min$ from 150°C to 300°C where the temperature was held stable for 23 min for films deposition, before cooling down at around $7.5°C/min$ and unloading at 150°C. Wafers from the second series were coated with a stack of Al_2O_3 deposited by plasma-assisted atomic layer deposition (ALD) and SiN_x deposited using an Oxford PlasmaLab PECVD system. The Al_2O_3 films were deposited at 175°C for around 40 min, whereas the SiN_x films were deposited at 400°C for around 8 min. After film deposition, the wafers were annealed in a nitrogen ambient at 425°C for 15 min to activate the surface passivation of the Al_2O_3 films. Both selected dielectric films provide excellent surface passivation with S_{eff} below $10cm/s$, confirmed with monocrystalline silicon control wafers.

Degradation was performed on a hotplate under illumination with a halogen lamp at around 2 sun light intensity. Rather than using 1 sun condition, we chose to use a slightly higher light intensity to accelerate the degradation [19]. The wafers were illuminated at 80°C and 145°C respectively. Before the degradation, the samples were annealed in the dark at 200°C for 15 min. The effective carrier lifetimes were measured at defined time steps during the degradation, using the quasi-steady-state photoconductance (QSSPC) technique [31] and photoluminescence (PL) imaging [32].

Moreover, the work also includes several p-type PERC solar cells made from Cz-Si, HP mc-Si and mono-like Si to show the detrimental impact of LeTID on finished cells. The solar cells were randomly selected from an industrial production line. The wafers used were sourced from the same suppliers, but taken from different ingots than the lifetime samples described above. The degradation treatment was carried out in a light-soaking chamber at around 65°C for 5 h under an irradiance level of 1 sun. The cell efficiency was measured before and after the degradation, using a solar simulator. Note the different degradation conditions used in the finished solar cells and the lifetime test samples mentioned above, as the degradations were performed with different equipment setups.

3. Results

Table 2 shows the degradation in the studied p-type PERC solar cells after 5 h of light soaking at 65°C under an irradiance level of 1 sun. Note that Table 2 only provides an illustration of the degradation trends, as the degradation maximum has not been achieved given the short illumination time. Nevertheless, the results clearly demonstrate that all three types of solar cells exhibit degradation behaviour under illumination. A relative degradation of 4.3% and 4.6% was observed on the HP mc-Si and Cz-Si PERC solar cells after light soaking. Surprisingly, the degradation was most severe on the mono-like Si PERC solar cells, with an average relative degradation of 9.1%. This is contrary to a previous study by Ramspeck et al. [4] who observed a smaller degradation on mono-like Si PERC solar cells compared to conventional mc-Si PERC solar cells. A possible explanation is that the two materials (mono-like Si and HP mc-Si) contain different impurity concentrations as they were grown by different manufacturers. However, we have observed a similar behaviour on solar cells made from HP mc-Si and mono-like Si materials grown by the same manufacturer (measurements not presented here). In any case, our results show that the degradation in

Table 1
Properties of materials studied in this work.

Material	Dopant	Resistivity (Ω cm)	$[O_i](cm^{-3})$
p-type HP mc-Si	Boron	1.7	1.7×10^{17}
n-type HP mc-Si	Phosphorus	2.1	NA
p-type mono-like Si	Boron	1.4	2.3×10^{17}
p-type Cz-Si	Boron	1.6	5.6×10^{17}

Table 2
Efficiency variation in p-type boron-doped PERC solar cells after 5 h of light soaking at ***65°C*** under an irradiance level of 1 sun.

Material	Number of cells	Avg. initial efficiency	Avg. final efficiency	Relative degradation
p-type HP mc-Si	4	19.0%	18.2%	4.3%
p-type mono-like Si	4	19.7%	17.9%	9.1%
p-type Cz-Si	5	20.9%	19.9%	4.6%

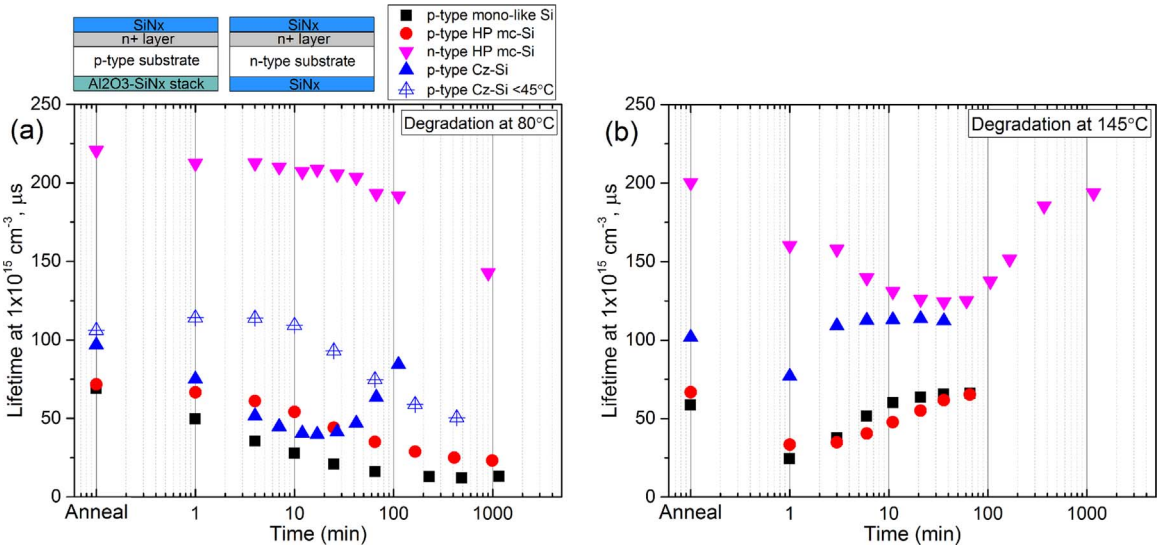

Fig. 1. Effective carrier lifetimes of cell pre-cursors as a function of time under 2 sun illumination at (a) 80 ℃ and (b) ***145℃***. All samples were fired in an industrial conveyor-belt furnace. The lifetimes are measured at an excess carrier density of $1\times10^{15}cm^{-3}$ by the QSSPC technique. All samples were annealed in the dark at ***200℃*** for 15 min before degradation. Hollow symbols in (a) represent the lifetimes of a p-type Cz-Si sample with degradation performed below 45 ℃.

mono-like Si solar cells can be even more severe than in Cz-Si solar cells.

Fig. 1 shows the measured effective lifetimes on cell pre-cursors as a function of degradation time. Also included in Fig. 1 is an n-type phosphorus-doped HP mc-Si sample which was treated similarly to the p-type cell pre-cursors, but passivated with different dielectric films. Overall, a reduction in lifetimes after illumination can be seen on all samples, including the p-type mono-like Si and the n-type HP mc-Si. While degradation occurs in all samples, the rate of degradation varies. The p-type Cz-Si sample exhibits the fastest degradation, owing to the faster reaction rate of the BO complex compared to LeTID. A lifetime recovery can also be seen in the p-type Cz-Si samples after 17 min of light soaking, due to regeneration of BO complex. Note that various works have also detected LeTID defects in Cz-Si [20,24]. Here, we are not able to confirm the presence of LeTID defects in the Cz-Si sample, as its influence is overshadowed by BO defects. However, we observe a similar extent of degradation in the Cz-Si sample when illuminated below 45°C, suggesting that the measured effective lifetimes of the studied Cz-Si samples are likely to be dominated by BO defects.

On the other hand, the degradation rate in n-type HP mc-Si is orders of magnitude slower than in the p-type mc-Si and mono-like Si samples. At 80°C, the lifetime reduction is not obvious within the first 100 min of illumination. Increasing the temperature to 145°C dramatically increases the reaction rate. For the n-type HP mc-Si, lifetime reduction is already noticeable after 1 min of illumination and a recovery of lifetime can be observed after 36 min. The result may suggest the presence of LeTID defects in n-type HP mc-Si.

In order to confirm whether the lifetime reduction in the p-type mono-like Si sample and the n-type HP mc-Si sample are caused by LeTID defects commonly observed on p-type mc-Si, the influence of the firing profile on the degradation behaviour are evaluated, as it has been reported that LeTID depends strongly on the firing conditions [10,14]. Fig. 2 compares the lifetime degradation on samples that have not been fired, and fired with different cooling profiles. All Cz-Si samples show a reduction in lifetimes after illumination. Comparing Figs. 1(a) and 2, it can be seen that the formation and passivation of the BO defect in Cz-Si is dramatically accelerated in the fired samples, but not significantly affected by the cooling profile at this temperature range, consistent with previous studies [33–35]. In contrast, only the fast-cooled mono-like Si and mc-Si samples degrade noticeably after light soaking. We note that for the p-type HP mc-Si, only a small amount of degradation can be detected. This could be due to the fact that the cooling rate applied is not as fast as the rapid cooling rate used in an industrial conveyor-belt furnace, meaning fewer defects are generated.

Our results are in line with previous work by Eberle et al. [14], and further demonstrate that LeTID can be activated by increasing the cooling rate alone, while keeping the ramp-up rate fixed. Moreover, our results suggest that the same defects could be responsible for the degradation in p-type and n-type cast-grown materials, as we observed a similar dependence of the degradation behaviour on the firing process.

We note that the p-type and n-type samples described above feature different passivating dielectric films on the rear surfaces, and the presence of n + layers on the front surfaces also limits the measured lifetime. To reduce the potential influence of surface recombination on the results, additional lifetime test samples were prepared. These samples received the same thermal treatments as the n-type samples mentioned above (phosphorus diffused and passivated with SiN_x), but had their dielectric films and the n + layers removed after firing in an industrial conveyor-belt furnace, before being re-coated with fresh dielectric films on both surfaces.

Fig. 3(a) shows the lifetimes of the SiN_x re-passivated samples during the degradation treatment. Plotted also in Fig. 3(a) are the lifetimes of a p-type FZ-Si and an n-type Cz-Si control samples with the same passivating films. It is important to consider the stability of the passivating films when evaluating bulk degradation [26,36–38]. The control samples were not fired, and hence should not be affected by LeTID. The control samples show a reduction in lifetimes after illumination of 1000 min, which is likely to be due to degradation in the passivation quality of the dielectric films [26,36,37]. The degradation in surface passivation has minimal impact on the p-type samples given their relatively lower bulk lifetimes, but can, to some extent, affect the measured lifetimes of the n-type HP mc-Si. Nevertheless, the degradation rate observed in the controls appears to be at least one order of magnitude slower than in the studied samples, indicating that the observed degradation in the studied samples is bulk related. In order to further discriminate the potential influence of surface recombination on the n-type HP mc-Si, we repeated the experiment with a different dielectric film (Al_2O_3-SiN_x stack) and raised the temperature to 145°C to accelerate the degradation. The result is shown in Fig. 3(b). No significant lifetime degradation can be observed in the controls within 1000 min of light soaking, whereas the lifetime in the n-type HP mc-Si drops considerably and recover afterwards, confirming that the degradation observed in n-type HP mc-Si is indeed a bulk effect.

Comparing Figs. 3(a) and 1(a), the degradation behaviour in the re-

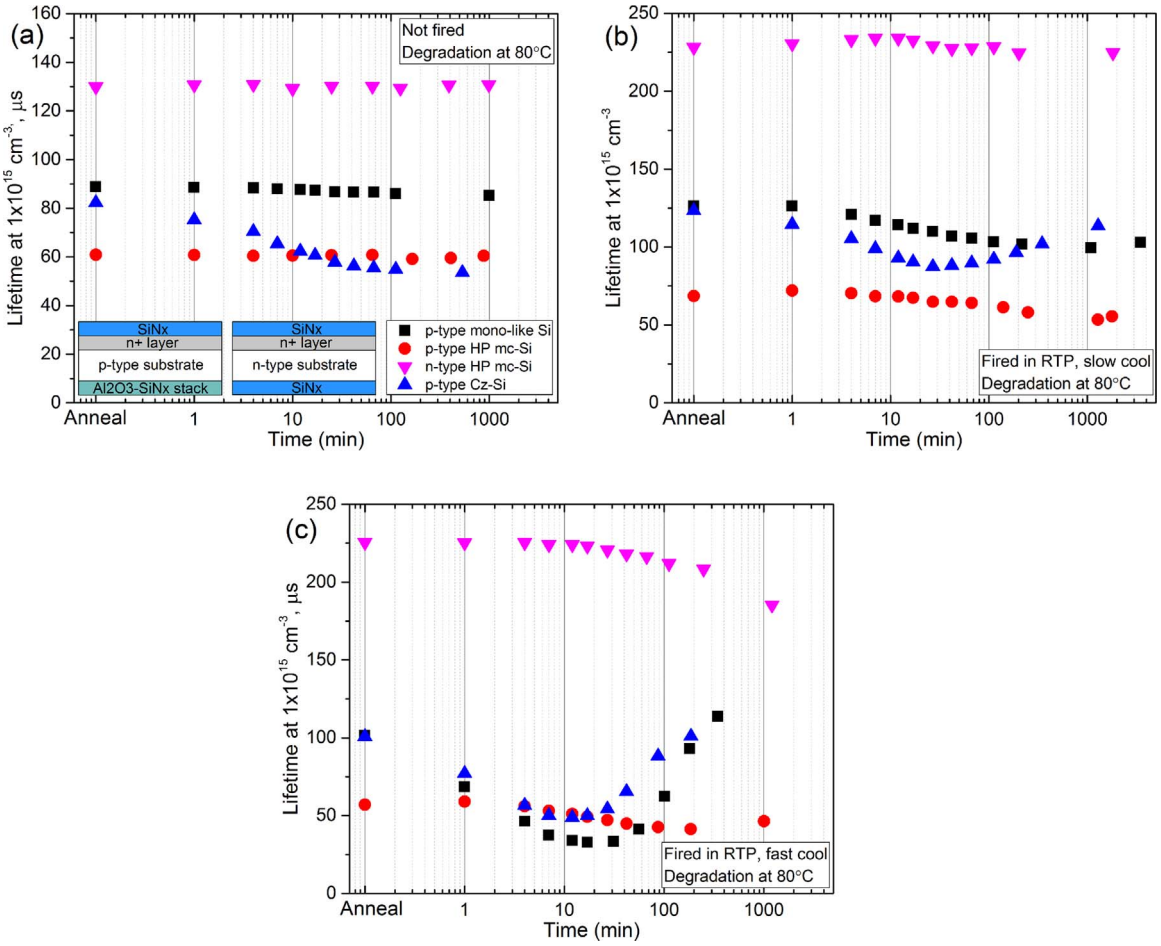

Fig. 2. Effective carrier lifetimes of cell pre-cursors as a function of time under 2 sun illumination at 80 ℃. The samples were (a) not fired, (b) fired at ***700℃*** for ***5s*** in a RTP furnace with slow ramp-down and (c) fired at ***700℃*** for ***5s*** in a RTP furnace with fast ramp-down. The lifetimes are measured at an excess carrier density of $1\times10^{15}cm^{-3}$ by QSSPC technique. Note the different lifetime scale used for (a).

passivated samples is similar to the cell pre-cursors discussed previously. Here, a larger degradation is observed in the re-passivated samples, most likely due to the fact that the measured effective lifetimes, in this case, are more sensitive to the bulk lifetimes, due to the absence of the n + layers, combined with the excellent surface passivation. The lifetime of the n-type HP mc-Si wafer, for example, reduces more than twofold (from around 2*ms* to below 1*ms*) after light soaking. Apart from the amplitude of the degradation, the rate of degradation also seems to be faster in the re-passivated samples. The faster degradation rate is probably caused by the higher injection levels

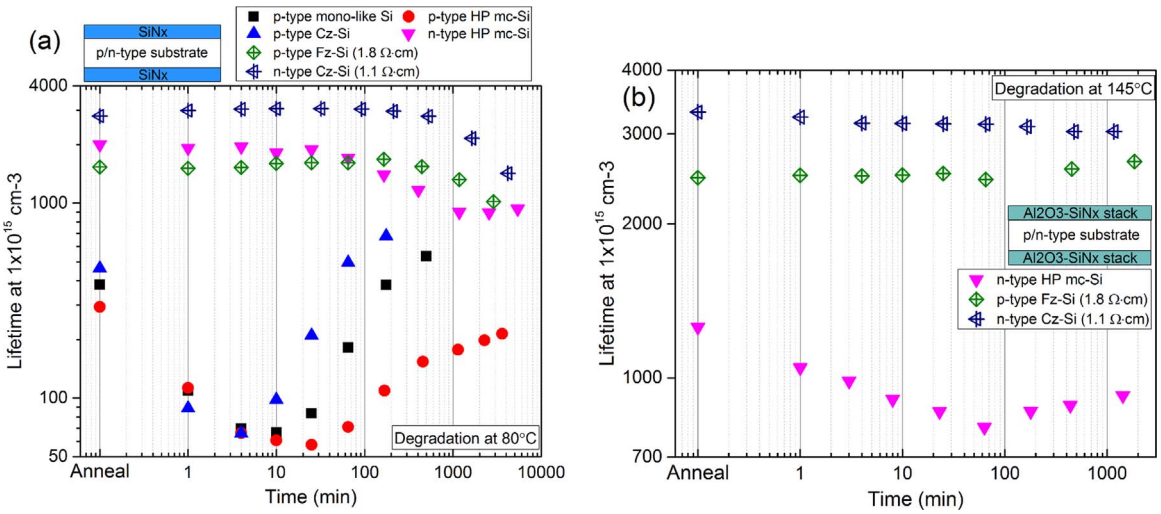

Fig. 3. (a) Effective carrier lifetimes of SiN_x passivated samples as a function of time under 2 sun illumination at ***80℃***. (b) Effective carrier lifetimes of Al_2O_3-SiN_x passivated samples as a function of time under 2 sun illumination at ***145℃***. All samples were coated with fresh dielectric films with S_{eff} below ***10cm/s*** after having their n + layers removed and their surfaces chemically polished. The lifetimes are measured at an excess carrier density of $1\times10^{15}cm^{-3}$ by QSSPC technique. Note the different logarithmic lifetime scales used for (a) and (b).

in the re-passivated samples as a result of their higher initial minority carrier lifetimes.

Comparing the measured lifetimes at the fully degraded state, n-type mc-Si exhibits substantially higher lifetimes than p-type mc-Si. This implies that n-type mc-Si features a lower normalised defect concentration [39], either due to a reduced defect concentration or the fact that the corresponding defects have a capture cross-section ratio greater than 1. Moreover, the significantly slower degradation rate in n-type mc-Si may suggest that the locations of the quasi fermi levels play a role in the formation of defects responsible for LeTID. For instance, various works have shown that the degradation time constant of the boron-oxygen complex depends on the hole concentration in both p-type and compensated n-type Cz-Si [40–42]. It is possible that a similar correlation could occur for LeTID in mc-Si, which would explain the slower degradation in n-type mc-Si materials. Further studies are needed to verify this hypothesis. We note that these results indicate that LeTID can potentially be more problematic in n-type mc-Si, as much longer times are needed for the defect deactivation, owing to its slow reaction rate.

It is important to consider the lateral inhomogeneity in mc-Si materials when evaluating the kinetics of LeTID. The reasons are several. First, mc-Si contains crystal defects such as grain boundaries and dislocations which exhibit different recombination properties compared to the intra-grain regions [43,44]. It is possible that different recombination sources at crystal defects and in intra-grain regions interact differently with the defects or precursors responsible for LeTID. Second, the degradation is highly unlikely to be uniform across an entire mc-Si wafer owing to the substantial lifetime variation across mc-Si wafers and the strong dependence of the degradation rate on injection level, as shown above and also in previous works [16–18,21]. We have observed a variation of more than 1 order of magnitude in the excess carrier density across the mc-Si wafers studied in this work under uniform illumination. Lastly, the amplitude of the degradation should also depend on the local lifetime. Higher lifetime areas such as the intra-grain regions should be, in principle, more susceptible to lifetime degradation in comparison with lower lifetime regions such as crystal defects, as the lifetime in the latter is strongly affected by other recombination mechanisms.

Fig. 4 shows calibrated PL lifetime images of the SiN_x re-passivated samples before and after the degradation treatment. Degradation occurs throughout the entire wafer in all samples, but is quite inhomogeneous, being particularly severe in regions surrounding recombination active crystal defects in p-type and n-type HP mc-Si. Similar observations have been reported in previous work [6,13,14]. One plausible explanation is that impurities or precursors responsible for LeTID could diffuse from crystal defects into the surrounding regions during the light soaking, leading to a faster degradation and a stronger reduction of lifetimes in those areas. If metal impurities are responsible, only fast diffusing species such as copper, cobalt and nickel, in principle, can contribute to such a large lateral diffusion at the studied temperatures and times. In contrast, certain inactive GBs in the p-type mc-Si sample, as highlighted in Fig. 4, seem to be less affected by the degradation. Bright regions or denuded zones can be observed around those GBs after light soaking. This phenomenon has also been reported by Luka et al. [45] and Selinger et al. [46].

4. Discussions

Various physical models have been proposed for LeTID. It is speculated that LeTID may originate from dissolution and reconfiguration of metal impurities that occurs during the firing process [12,14,47]. This hypothesis is supported by the fact that substantial LeTID can only be detected after rapid quenching, which is known to affect the forms and structures of metal precipitates in mc-Si [48]. This hypothesis is consistent with our results given that the responsible metal impurities are likely to be diffused from the crucible walls and coatings used in the ingot growth process, and so should be present in all of the cast-grown mc-Si samples studied in this work, including the

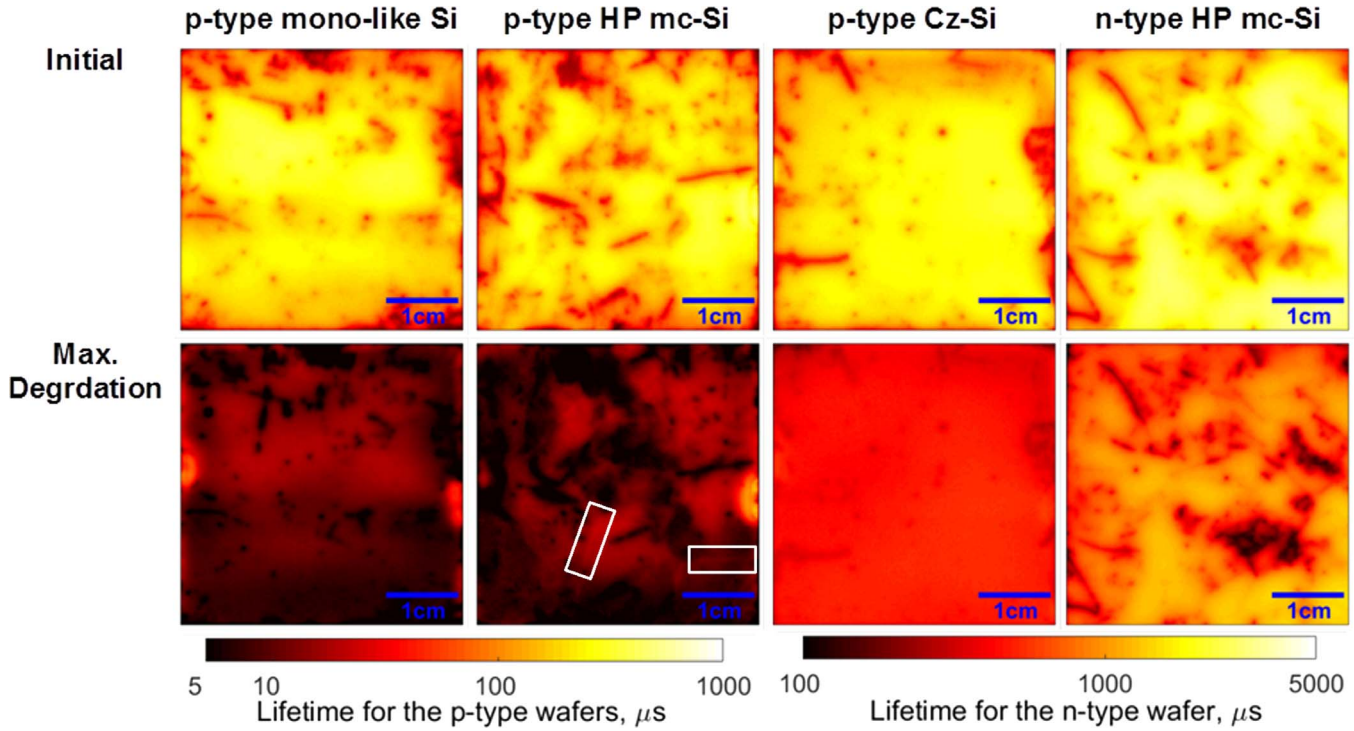

Fig. 4. Calibrated PL lifetime images of the SiN_x passivated samples before and after degradation treatment. Maximum degradation was achieved after approximately 10, 25, 4 and 2600 min of illumination at ***80°C*** for the p-type mono-like Si, the p-type HP mc-Si, the p-type Cz-Si and the n-type HP mc-Si respectively. PL images were taken at 0.1 sun condition, which corresponds to an injection level close to maximum power in a working solar cell. A logarithmic lifetime scale is used in the figure. Note the different lifetime scales used for the p-type and n-type samples.

p-type mono-like Si and the n-type HP mc-Si, which show LeTID behaviours after a fast-firing process. Researchers have indeed shown that copper contamination can cause LID in silicon [49–51]. However, if copper is responsible for the LID effect observed in this work, it is not clear why we observe a much slower defect reaction in the n-type cast material than in p-type. Moreover, various research groups have also detected LeTID-like behaviour in p-type Cz-Si [20,24] and FZ-Si [25–27], which should, in principle, contain considerably less metal impurities.

On the other hand, several authors have suggested the involvement of hydrogen, which can form parts of the detrimental LeTID complex [12,14,47], passivate the LeTID complex [7,47], or even serve both roles during the degradation and regeneration [52]. This model may explain the disparity in the degradation rate in p-type and n-type mc-Si studied in this work, as it has been shown that the diffusivity of hydrogen varies in p-type and n-type silicon [53–56]. The two models described here do not necessarily contradict with each other, and it is possible that both metal impurities and hydrogen play a role in LeTID.

It should be mentioned that all samples studied in this work were annealed in the dark at 200°C for 15 min before light soaking. It has been reported that dark annealing can change the kinetics of LeTID [45,52,57]. This can affect some of the results presented in this work qualitatively, but is unlikely to alter the overall conclusions.

5. Conclusions

Our results demonstrate the fundamental differences in the defect formation mechanism between the BO complex in Cz-Si and LeTID in mc-Si. While all Cz-Si samples degrade after light soaking, only the mc-Si samples fired with a rapid cool-down show noticeable degradation. In addition to conventional p-type mc-Si, LeTID is also observed on p-type mono-like Si and n-type mc-Si. Interestingly, the degradation rate in n-type HP mc-Si is found to be orders of magnitude slower than in p-type mc-Si, implying that the defect formation could be affected by the positions of the quasi fermi levels, which can affect the charge states of impurities. Furthermore, lifetime images reveal that the degradation seems to be most severe in regions surrounding crystal defects. These findings could serve to guide further studies to identify the root causes of LeTID, and correspondingly develop effective mitigation solutions.

Acknowledgments

This work has been supported by the Australian Renewable Energy Agency (ARENA) through project RND009. H. C. Sio would like to thank S. P. Phang at the Australian National University and M. A. Jensen at Massachusetts Institute of Technology for fruitful discussions.

References

[1] J. Schmidt, A. Cuevas, Electronic properties of light-induced recombination centers in boron-doped Czochralski silicon, J. Appl. Phys. 86 (1999) 3175–3180.
[2] S.W. Glunz, S. Rein, J.Y. Lee, W. Warta, Minority carrier lifetime degradation in boron-doped Czochralski silicon, J. Appl. Phys. 90 (2001) 2397–2404.
[3] K. Bothe, R. Sinton, J. Schmidt, Fundamental boron–oxygen-related carrier lifetime limit in mono- and multicrystalline silicon, Prog. Photovolt.: Res. Appl. 13 (2005) 287–296.
[4] K. Ramspeck, S. Zimmermann, H. Nagel, A. Metz, Y. Gassenbauer, B. Birkmann, , *et al.*, "Light induced degradation of rear passivated mc-si solar cells," in: Proceedings of the 27th European Photovoltaic Solar Energy Conference and Exhibition, Frankfurt, Germany, 2012.
[5] F. Fertig, K. Krauß, S. Rein, Light-induced degradation of PECVD aluminium oxide passivated silicon solar cells, Phys. Status Solidi (RRL) – Rapid Res. Lett. 9 (2015) 41–46.
[6] K. Krauss, F. Fertig, D. Menzel, S. Rein, Light-induced degradation of silicon solar cells with aluminium oxide passivated rear side,", Energy Procedia 77 (2015) 599–606.
[7] K. Nakayashiki, J. Hofstetter, A.E. Morishige, T.T.A. Li, D.B. Needleman, M.A. Jensen, et al., Engineering Solutions and root-cause analysis for light-induced degradation in p-type multicrystalline silicon PERC modules, IEEE J. Photovolt. 6 (2016) 860–868.
[8] M. Padmanabhan, K. Jhaveri, R. Sharma, P.K. Basu, S. Raj, J. Wong, et al., Light-induced degradation and regeneration of multicrystalline silicon Al-BSF and PERC solar cells, Phys. Status Solidi (RRL) – Rapid Res. Lett. 10 (2016) 874–881.
[9] F. Kersten, F. Fertig, K. Petter, B. Klöter, E. Herzog, M.B. Strobel, et al., System performance loss due to LeTID, Energy Procedia (2017).
[10] C.E. Chan, D.N.R. Payne, B.J. Hallam, M.D. Abbott, T.H. Fung, A.M. Wenham, et al., Rapid stabilization of high-performance multicrystalline p-type silicon PERC cells, IEEE J. Photovolt. 6 (2016) 1473–1479.
[11] F. Kersten, J. Heitmann, J.W. Müller, Influence of Al_2O_3 and SiNx passivation layers on LeTID, Energy Procedia 92 (2016) 828–832.
[12] D. Bredemeier, D. Walter, S. Herlufsen, J. Schmidt, Lifetime degradation and regeneration in multicrystalline silicon under illumination at elevated temperature, AIP Adv. 6 (2016) 035119.
[13] A. Zuschlag, D. Skorka, G. Hahn, Degradation and regeneration in mc-Si after different gettering steps, Prog. Photovolt.: Res. Appl. (2016).
[14] R. Eberle, W. Kwapil, F. Schindler, M.C. Schubert, S.W. Glunz, Impact of the firing temperature profile on light induced degradation of multicrystalline silicon, Phys. Status Solidi (RRL) – Rapid Res. Lett. (2016).
[15] D. Bredemeier, D. Walter, J. Schmidt, Light-induced lifetime degradation in high-performance multicrystalline silicon: detailed kinetics of the defect activation, Sol. Energy Mater. Sol. Cells 173 (2017) 2–5.
[16] W. Kwapil, T. Niewelt, M.C. Schubert, Kinetics of carrier-induced degradation at elevated temperature in multicrystalline silicon solar cells, Sol. Energy Mater. Sol. Cells 173 (2017) 80–84.
[17] F. Kersten, P. Engelhart, H.-C. Ploigt, A. Stekolnikov, T. Lindner, F. Stenzel, et al., Degradation of multicrystalline silicon solar cells and modules after illumination at elevated temperature, Sol. Energy Mater. Sol. Cells 142 (2015) 83–86.
[18] F. Kersten, P. Engelhart, H.C. Ploigt, A. Stekolnikov, T. Lindner, F. Stenzel, et al., "A new mc-Si degradation effect called LeTID," in: Proceedings of the Photovoltaic Specialist Conference (PVSC) IEEE 42nd, 2015, pp. 1–5.
[19] D.N.R. Payne, C.E. Chan, B.J. Hallam, B. Hoex, M.D. Abbott, S.R. Wenham, et al., Acceleration and mitigation of carrier-induced degradation in p-type multi-crystalline silicon, Phys. Status Solidi (RRL) – Rapid Res. Lett. 10 (2016) 237–241.
[20] D. Chen, M. Kim, B.V. Stefani, B.J. Hallam, M.D. Abbott, C.E. Chan, et al., Evidence of an identical firing-activated carrier-induced defect in monocrystalline and multicrystalline silicon, Sol. Energy Mater. Sol. Cells 172 (2017) 293–300.
[21] D.N.R. Payne, C.E. Chan, B.J. Hallam, B. Hoex, M.D. Abbott, S.R. Wenham, et al., Rapid passivation of carrier-induced defects in p-type multi-crystalline silicon, Sol. Energy Mater. Sol. Cells 158 (2016) 102–106.
[22] K. Krauß, A.A. Brand, F. Fertig, S. Rein, J. Nekarda, Fast Regeneration processes to avoid light-induced degradation in multicrystalline silicon solar cells, IEEE J. Photovolt. 6 (2016) 1427–1431.
[23] B.J. Hallam, P.G. Hamer, S.R. Wenham, M.D. Abbott, A. Sugianto, A.M. Wenham, et al., Advanced Bulk defect passivation for silicon solar Cells, IEEE J. Photovolt. 4 (2014) 88–95.
[24] F. Fertig, R. Lantzsch, A. Mohr, M. Schaper, M. Bartzsch, D. Wissen, et al., Mass production of p-type Cz silicon solar cells approaching average stable conversion efficiencies of 22%, Energy Procedia 124 (2017) 338–345.
[25] D. Sperber, A. Herguth, G. Hahn, A 3-state defect model for light-induced degradation in boron-doped float-zone silicon, Phys. Status Solidi (RRL) – Rapid Res. Lett. 11 (2017) 1600408.
[26] D. Sperber, A. Heilemann, A. Herguth, G. Hahn, Temperature and light-induced changes in bulk and passivation quality of boron-doped float-zone silicon coated With SiNx: h, Ieee J. Photovolt. 7 (2017) 463–470.
[27] T. Niewelt, M. Selinger, N.E. Grant, W. Kwapil, J.D. Murphy, M.C. Schubert, Light-induced activation and deactivation of bulk defects in boron-doped float-zone silicon, J. Appl. Phys. 121 (2017) 185702.
[28] K. Kutsukake, N. Usami, Y. Ohno, Y. Tokumoto, I. Yonenaga, Mono-Like silicon growth using functional grain boundaries to limit area of multicrystalline Grains, IEEE J. Photovolt. 4 (2014) 84–87.
[29] T. Isao, J. Supawan, I. Taisho, U. Noritaka, Seed manipulation for artificially controlled defect technique in new growth method for quasi-monocrystalline Si ingot based on casting, Appl. Phys. Express 8 (2015) 105501.
[30] D. Macdonald, J. Tan, T. Trupke, Imaging interstitial iron concentrations in boron-doped crystalline silicon using photoluminescence, J. Appl. Phys. 103 (2008) 073710.
[31] R.A. Sinton, A. Cuevas, M. Stuckings, "Quasi-steady-state photoconductance, a new method for solar cell material and device characterization," in: Proceedings of the 25th IEEE Photovoltaic Specialists Conference, 1996 pp. 457–460.
[32] T. Trupke, R.A. Bardos, M.C. Schubert, W. Warta, Photoluminescence imaging of silicon wafers, Appl. Phys. Lett. 89 (2006) 044107.
[33] S. Wilking, A. Herguth, G. Hahn, Influence of hydrogen on the regeneration of boron-oxygen related defects in crystalline silicon, J. Appl. Phys. 113 (2013) 194503.
[34] S. Wilking, S. Ebert, A. Herguth, G. Hahn, Influence of hydrogen effusion from hydrogenated silicon nitride layers on the regeneration of boron-oxygen related defects in crystalline silicon, J. Appl. Phys. 114 (2013) 194512.
[35] N. Nampalli, B. Hallam, C. Chan, M. Abbott, S. Wenham, Evidence for the role of hydrogen in the stabilization of minority carrier lifetime in boron-doped Czochralski silicon, Appl. Phys. Lett. 106 (2015) 173501.
[36] D. Sperber, F. Furtwängler, A. Herguth, G. Hahn, "On the stability of dielectric passivation layers under illumination and temperature treatment," in: Proceedings of the 32nd European Photovoltaic Solar Energy Conference and Exhibition, 2016, pp. 523–526.
[37] D. Sperber, A. Herguth, G. Hahn, Instability of dielectric surface passivation quality at elevated temperature and illumination, Energy Procedia 92 (2016) 211–217.
[38] T. Niewelt, W. Kwapil, M. Selinger, A. Richter, M.C. Schubert, Long-Term stability

of aluminum oxide based surface passivation schemes under illumination at elevated temperatures, IEEE J. Photovolt. 7 (2017) 1197–1202.
[39] S.W. Glunz, S. Rein, W. Warta, J. Knobloch, W. Wettling, Degradation of carrier lifetime in Cz silicon solar cells, Sol. Energy Mater. Sol. Cells 65 (2001) 219–229.
[40] V.V. Voronkov, R. Falster, K. Bothe, B. Lim, J. Schmidt, Lifetime-degrading boron-oxygen centres in p-type and n-type compensated silicon, J. Appl. Phys. 110 (2011) 063515.
[41] J. Schön, T. Niewelt, J. Broisch, W. Warta, M.C. Schubert, Characterization and modelling of the boron-oxygen defect activation in compensated n-type silicon, J. Appl. Phys. 118 (2015) 245702.
[42] T.U. Nærland, H. Haug, H. Angelskår, R. Søndenå, E.S. Marstein, L. Arnberg, Studying light-induced degradation by lifetime decayanalysis: excellent fit to solution of simple second-order rate equation, IEEE J. Photovolt. 3 (2013) 1265–1270.
[43] H.C. Sio, D. Macdonald, Direct comparison of the electrical properties of multicrystalline silicon materials for solar cells: conventional p-type, n-type and high performance p-type, Sol. Energy Mater. Sol. Cells 144 (2016) 339–346.
[44] H.C. Sio, S.P. Phang, P. Zheng, Q. Wang, W. Chen, H. Jin, et al., Recombination sources in p-type high performance multicrystalline silicon, Jpn. J. Appl. Phys. (2017).
[45] T. Luka, S. Großer, C. Hagendorf, K. Ramspeck, M. Turek, Intra-grain versus grain boundary degradation due to illumination and annealing behavior of multi-crystalline solar cells, Sol. Energy Mater. Sol. Cells 158 (2016) 43–49.
[46] M. Selinger, W. Kwapil, F. Schindler, K. Krauß, F. Fertig, B. Michl, et al., Spatially resolved analysis of light induced degradation of multicrystalline PERC solar cells, Energy Procedia 92 (2016) 867–872.
[47] M.A. Jensen, A.E. Morishige, J. Hofstetter, D.B. Needleman, T. Buonassisi, Evolution of LeTID defects in p-Type Multicrystalline Silicon During Degradation and Regeneration, IEEE J. Photovolt. 7 (2017) 980–987.
[48] T. Buonassisi, A.A. Istratov, M.D. Pickett, M. Heuer, J.P. Kalejs, G. Hahn, et al., Chemical natures and distributions of metal impurities in multicrystalline silicon materials, Prog. Photovolt.: Res. Appl. 14 (2006) 513–531.
[49] J. Lindroos, H. Savin, Review of light-induced degradation in crystalline silicon solar cells, Sol. Energy Mater. Sol. Cells 147 (2016) 115–126.
[50] J. Lindroos, Y. Boulfrad, M. Yli-Koski, H. Savin, Preventing light-induced degradation in multicrystalline silicon, J. Appl. Phys. 115 (2014) 154902.
[51] S. Dubois, T. Turmagambetov, J.-P. Garandet, H. Lignier, N. Enjalbert, Influence of the solar cells metallization firing treatment on carrier recombination and trapping in copper contaminated multicrystalline silicon: new insights into the role of the phosphorus-rich layers, Sol. Energy Mater. Sol. Cells 157 (2016) 558–564.
[52] C. Chan, T.H. Fung, M. Abbott, D. Payne, A. Wenham, B. Hallam, et al., Modulation of carrier-induced defect kinetics in multi-crystalline silicon PERC cells through dark Annealing, Sol. RRL 1 (2017) 1600028.
[53] C.G. Van de Walle, P.J.H. Denteneer, Y. Bar-Yam, S.T. Pantelides, Theory of hydrogen diffusion and reactions in crystalline silicon, Phys. Rev. B 39 (1989) 10791–10808.
[54] K.J. Chang, D.J. Chadi, Hydrogen bonding and diffusion in crystalline silicon, Phys. Rev. B 40 (1989) 11644–11653.
[55] R. Rizk, P. De Mierry, D. Ballutaud, M. Aucouturier, D. Mathiot, Hydrogen diffusion and passivation processes in p-and n-type crystalline silicon, Phys. Rev. B 44 (1991) 6141.
[56] D. Mathiot, Modeling of hydrogen diffusion in n- and p-type silicon, Phys. Rev. B 40 (1989) 5867–5870.
[57] T.H. Fung, C.E. Chan, B.J. Hallam, D.N.R. Payne, M.D. Abbott, S.R. Wenham, Impact of annealing on the formation and mitigation of carrier-induced defects in multi-crystalline silicon, Energy Procedia 124 (2017) 726–733.